



Published in final edited form as:

Heart Rhythm. 2010 January ; 7(1): 88–95. doi:10.1016/j.hrthm.2009.09.018.

Mechanisms of sinoatrial node dysfunction in a canine model of pacing-induced atrial fibrillation

Boyoung Joung, MD, PhD, Shien-Fong Lin, PhD, Zhenhui Chen, PhD, Patrick S. Antoun, MD, Mitsunori Maruyama, MD, Seongwook Han, MD, PhD, Gianfranco Piccirillo, MD, PhD, Marcelle Stucky, BS, Douglas P. Zipes, MD, FHRS, Peng-Sheng Chen, MD, FHRS, and Mithilesh Kumar Das, MD

Krannert Institute of Cardiology and the Division of Cardiology, Department of Medicine, Indiana University School of Medicine, Indianapolis, Indiana

Abstract

BACKGROUND—The mechanism of sinoatrial node (SAN) dysfunction in atrial fibrillation (AF) is unclear.

OBJECTIVE—The purpose of this study was to test the hypothesis that defective spontaneous sarcoplasmic reticulum (SR) Ca^{2+} release (Ca^{2+} clock) is in part responsible for SAN dysfunction in AF.

METHODS—Arrhythmic events and SAN function were evaluated in pacing-induced AF dogs ($n = 7$) and in normal dogs ($n = 19$) with simultaneous intracellular calcium (Ca_i) and membrane potential recording.

RESULTS—AF dogs had frequent sinus pauses during Holter monitoring. Isolated right atrium (RA) from AF dogs showed slower heart rate ($P = .001$), longer SAN recovery time ($P = .001$), and longer sinoatrial conduction time ($P = .003$) than normal. In normal RAs, isoproterenol 0.3 and 1 $\mu\text{mol/L}$ increased heart rate by 96% and 105%, respectively. In contrast, in RAs from AF dogs, isoproterenol increased heart rate by only 60% and 72%, respectively. Isoproterenol induced late diastolic Ca_i elevation (LDCAE) at superior SAN in all 19 normal RAs but in only 3 of 7 AF RAs ($P = .002$). In AF RAs without LDCAE ($n = 4$), heart rate increased by the acceleration of ectopic foci. Caffeine (20 mmol/L) injection increased heart rate with LDCAE in all 6 normal RAs but did not result in LDCAE in any of the 5 AF RAs ($P = .002$). Type 2 ryanodine receptor (RyR2) in the superior SAN of AF dogs was decreased to 33% of normal ($P = .02$).

CONCLUSION—SAN dysfunction in AF is associated with Ca^{2+} clock malfunction, characterized by unresponsiveness to isoproterenol and caffeine and down-regulation of RyR2 in SAN.

Keywords

Atrial fibrillation; Calcium; Sarcoplasmic reticulum; Sinoatrial node dysfunction

Introduction

Atrial fibrillation (AF) is associated with significant electrophysiologic and structural remodeling¹ and often is associated with sick sinus (tachybrady) syndrome.^{2,3} In dogs,

persistent (>2 weeks) rapid atrial pacing and chronic AF resulted in sinoatrial node (SAN) dysfunction, as evidenced by prolongation of SAN recovery time (SNRT) and decreases in intrinsic heart rates.⁴ Comparable data in humans have been reported.^{2,5,6} Furthermore, successful catheter ablation of AF may be followed by significant improvements in SAN function.³ These findings suggest that rapid activation during AF can cause reversible impairment of SAN. However, the cellular mechanism of SAN dysfunction in AF remains unclear. Spontaneous diastolic depolarization of SAN cells periodically initiates action potentials to set the rhythm of the heart. The mechanism of spontaneous diastolic depolarization traditionally has been attributed to a “voltage clock” mechanism, mediated by voltage-sensitive membrane ion currents, such as the hyperpolarization-activated pacemaker current (I_f).^{7,8} Recently, the “ Ca^{2+} clock” has been proposed as a complementary mechanism of SAN automaticity.^{9–14} The Ca^{2+} clock is mediated by rhythmic spontaneous sarcoplasmic reticulum (SR) Ca^{2+} release, which in turn activates Na^+/Ca^{2+} exchanger current (I_{NCX}) and causes diastolic depolarization.^{9–14} Using simultaneous membrane potential (V_m) and intracellular calcium (Ca_i) mapping, our laboratory recently demonstrated that acceleration of the Ca^{2+} clock in the superior SAN plays an important role in sinus acceleration during beta-adrenergic stimulation, interacting synergistically with the membrane clock in an isolated, Langendorff-perfused right atrium (RA) model.¹⁵ The aim of the present study was to evaluate Ca_i dynamics in intact SANs of dogs with pacing-induced AF by using simultaneous V_m and Ca_i mapping. The results were used to test the hypothesis that a defective Ca^{2+} clock underlies the mechanism of SAN dysfunction in a canine model of pacing-induced AF.

Methods

All animal study protocols were approved by the Institutional Animal Care and Use Committee of Indiana University School of Medicine and the Methodist Research Institute. Pacing-induced AF was produced in 7 adult mongrel dogs (weight 25–30 kg) using previously described techniques.⁴ Ambulatory Holter recordings were obtained for 48 hours in dogs numbered 3 through 7. The dogs then were continuously paced at an atrial rate of 640 bpm for at least an additional 16 days (mean 21 ± 4 days, range 16–26 days) before sacrifice (Figure 1).

We studied isolated RA from 7 dogs with pacing-induced AF. The results were compared with results from 19 normal dogs. The data from 11 of the 19 normal dogs were included in a report published previously.¹⁵ To assess SAN function, SNRT and corrected SNRT (cSNRT) were determined in isolated RAs. Simultaneous V_m and Ca_i mapping was performed using previously described techniques.¹⁵ After dual V_m and Ca_i optical mapping of baseline spontaneous heart beats, pharmacologic intervention was performed. These interventions included isoproterenol infusion of $1 \mu\text{mol/L}$ in all RAs and a bolus injection of 2 mL caffeine (20 mmol/L) in 7 normal and 5 AF dog RAs. The heart rate response to isoproterenol (0.01, 0.03, 0.1, 0.3, 1, 3, 10 $\mu\text{mol/L}$) was tested in 7 normal and all 7 AF RAs. Expression levels of type 2 ryanodine receptor (RyR2), sarcoplasmic reticulum Ca^{2+} -ATPase 2a (SERCA2a), and phospholamban were evaluated in superior SAN of normal and AF dogs.

Data are expressed as mean \pm SEM. Student's t-tests with Bonferroni correction were used to compare the means of two numeric values. Pearson Chi-square tests were used to compare two categorical variables. The repeated-measures analysis of variance model was used to compare isoproterenol-induced heart rate response between AF and control dogs. $P < .05$ was considered significant. An expanded methods section is available in the Online Data Supplement.

Results

Evidence of atrial arrhythmia *in vivo*

In all rapid atrial pacing dogs, the development of spontaneous AF was confirmed by interrogation of the pacemaker during the monitoring period. Figure 2A shows an episode of AF obtained by interrogation of the implanted atrial pacemaker during the monitoring period. The average number and duration of spontaneous AF were 4.2 ± 2.4 times and 211.8 ± 325.6 minutes during the monitoring period for 24 hours, respectively. One of the 5 AF dogs had persistent AF during Holter monitoring. In the remaining 4 dogs, Holter monitoring documented 16 ± 23 paroxysmal AF episodes (mean duration 9 ± 20 minutes). During sinus rhythm, AF dogs had 347 ± 319 (range 4–634) episodes of prolonged sinus pauses (>3 seconds) with a mean duration of 3.3 ± 0.7 seconds.

Evidence of atrial arrhythmia *in vitro*

All 7 AF dogs developed spontaneous AF during the second surgery, whereas none of the 19 normal dogs developed AF ($P = .001$). AF was terminated spontaneously during Langendorff-perfusion in 6 RA preparations from AF dogs. Cardioversion was needed in one AF RA. After termination of AF, RAs from AF dogs had slower heart rates (72 ± 13 bpm vs 96 ± 16 bpm; $P = .001$), longer SNRT ($1,180 \pm 234$ ms vs 935 ± 170 ms; $P = .02$), and longer cSNRT (344 ± 98 ms vs 203 ± 72 ms; $P = .003$) than did those from normal dogs (Supplementary Figure 1A). Action potential duration measured to 90% repolarization (APD_{90}) was significantly shorter in AF dogs than in normal dogs (196 ± 23 ms vs 290 ± 40 ms; $P = .001$; Supplementary Figure 1B). SAN conduction time (SACT) was calculated based on the method proposed by Narula et al¹⁶ and was found to be longer in AF dogs than in control dogs (179 ± 49 ms vs 112 ± 39 ms; $P = .003$).

Baseline leading pacemaker site of RAs from normal dogs ($n = 19$) was located at inferior and middle SANs in 8 and 11 dogs, respectively. RAs from AF dogs ($n = 7$) had inferior and middle SANs as the leading pacemaker site in 4 and 3 dogs, respectively. The distribution of baseline leading pacemaker site showed no difference between AF and normal dogs ($P = .67$). None of the AF dogs showed late diastolic Ca_i elevation (LDCAE) at baseline, whereas 4 (21%) normal dogs showed small LDCAE at inferior SAN ($P = .55$).

Impaired heart rate response to beta-adrenergic stimulation in AF dogs

Figure 3 shows the isoproterenol dose–response curve of heart rate obtained from RAs of 7 normal and 7 AF dogs. In normal dogs, isoproterenol dosages of 0.3 and 1 $\mu\text{mol/L}$ increased heart rate to 152 ± 32 bpm (96%) and 161 ± 20 bpm (105%), respectively. In contrast, the heart rate of AF dogs during isoproterenol infusion increased to only 116 ± 31 bpm (60%) and 125 ± 24 bpm (72%), respectively. Compared with normal dogs, heart rate during isoproterenol infusion was slower in AF dogs, with a rightward shift of the heart rate response curve ($P = .03$).

Impaired LDCAE of SAN after beta-adrenergic stimulation in AF dogs

Figure 4 shows the typical isoproterenol response of RAs from normal dogs. Isoproterenol infusion of 0.3 $\mu\text{mol/L}$ increased heart rate to 168 bpm (97%) from 86 bpm and shifted the leading pacemaker site to superior SAN (Figure 4C(a)). A robust LDCAE (arrows in Ca_i tracing of Figure 4C(b)) occurred at the leading pacemaker site of superior SAN. This finding was consistently observed in all 19 normal RAs during isoproterenol infusion. However, only 3 of 7 RAs from AF dogs showed LDCAE and a shift of the leading pacemaker site during isoproterenol infusion ($P = .002$).

Figure 5 shows the isoproterenol response pattern in 4 of 7 AF RAs without LDCAE. During isoproterenol infusion of 0.3 $\mu\text{mol/L}$, heart rate increased to 95 bpm from 70 bpm. After increasing the isoproterenol dose to 1.0 $\mu\text{mol/L}$, heart rate was increased by acceleration of the ectopic focus from inferior RA (Figure 5C(a)). The Ca_i tracing showed no LDCAE anywhere in the mapped region with isoproterenol dose ranging from 0.01 to 10 $\mu\text{mol/L}$ (Figure 5C(b)).

Figure 6A shows the isoproterenol response pattern observed in 3 AF RAs that had LDCAE transiently. LDCAE was observed at the mid SAN during isoproterenol infusion of 0.1 $\mu\text{mol/L}$ (arrows in Ca_i tracing of Figure 6A(b)). With the increase of isoproterenol, LDCAE disappeared. The leading pacemaker sites shifted to inferior RA (Figure 6A(c)).

Impaired LDCAE after caffeine injection in AF dogs

Figure 6B(a) shows the typical caffeine response in normal RA. Caffeine injection increased heart rate to 171 ± 21 bpm (by 101%) from baseline of 86 ± 10 bpm and shifted the leading pacemaker site to superior SAN with concomitant LDCAE (arrows in Figure 6B(a)) in all 6 normal dogs. However, caffeine did not result in LDCAE or a shift of the leading pacemaker site in any of the 5 AF dogs ($P = .002$). Caffeine increased heart rate to 137 ± 18 bpm (99%) from baseline of 69 ± 10 bpm. There was an acceleration of ectopic focus from inferior RA (Figure 6B(b)) during caffeine injection. Mean maximum heart rate after caffeine injection was higher in normal dogs than in AF dogs ($P = .02$).

Leading pacemaker sites during heart rate acceleration

Figure 7 shows the origin of heart rhythm during acceleration of heart rate in each of the 7 AF RAs. In 4 AF RAs without LDCAE, heart rate was increased by acceleration of the ectopic focus or inferior SAN (black arrow in Figure 6A). In contrast, 3 AF RAs showed heart rate increase with transient LDCAE at mid SAN (red arrows in Figure 7B). Further increase of isoproterenol dosage moved the leading pacemaker sites to either inferior SAN or ectopic foci outside the mapped region.

Impaired LDCAE, Ca_i upstroke, and Ca_i relaxation in AF dogs

The slope of LDCAE at superior SAN progressively increased with higher doses of isoproterenol in normal dogs but was significantly impaired in AF dogs. We designate the maximum amplitude of Ca_i as 1 arbitrary unit (AU) (Figure 4A). During isoproterenol infusion, the slope of LDCAE of normal dogs increased from 0 AU/s to 2.0 ± 1.1 AU/s and 2.9 ± 1.3 AU/s at heart rates of 120–139 bpm and 140–159 bpm, respectively. In contrast, the slope of LDCAE of AF dogs increased from 0 AU/s to only 0.3 ± 0.8 AU/s ($P = .001$) and 0.5 ± 0.5 AU/s ($P = .001$), at the same respective heart rate, during isoproterenol infusion (Figure 8A(a)).

The slope of the Ca_i upstroke at the superior SAN was significantly lower in AF dogs than in normal dogs at baseline (7.9 ± 2.3 AU/s vs 12.2 ± 3.8 AU/s; $P = .02$) and during isoproterenol infusion (Figure 8A(b)).

Compared to normal dogs, superior SANs from AF dogs showed significantly longer 90% Ca_i relaxation time at baseline (420 ± 83 ms vs 265 ± 44 ms; $P = .001$). During isoproterenol infusion, the 90% Ca_i relaxation time of normal SANs decreased to 179 ± 23 ms and 153 ± 14 ms at heart rates of 120–139 bpm and 140–159 bpm, respectively. In contrast, the 90% Ca_i relaxation time of AF SANs decreased to only 207 ± 25 ms ($P = .02$) and 188 ± 29 ms ($P = .003$), at the same respective heart rate, during isoproterenol infusion (Figure 8A(c)). Data on LDCAE, Ca_i upstroke, and 90% Ca_i relaxation time measured from middle SAN, inferior SAN, and RA are presented in Supplementary Figure 2.

RyR2, SERCA2a, and phospholamban in SAN of normal and AF dogs

After optical mapping experiments, expression of RyR2, SERCA2a, and phospholamban at SAN was determined. In AF dogs, expression of RyR2 in the superior SAN was decreased to 33% of normal dogs ($P = .02$), whereas SERCA2a expression level remained unchanged at $100\% \pm 9\%$ ($P = .90$; Figure 8B(a)). Expression of phospholamban in AF dogs was reduced to $71\% \pm 8\%$ of normal dogs ($P = .41$; Figure 8B(b)).

Discussion

Major findings

A major finding of this study is that isoproterenol-induced LDCAE is severely impaired in the superior SAN of AF dogs. These changes were associated with significantly reduced RyR2 expression in the superior SAN. Due to an inability to develop LDCAE in the superior SAN, acceleration of heart rate was impaired and the superior SAN could not serve as the leading pacemaker site. These findings suggest that a defective Ca^{2+} clock at the superior SAN is in part responsible for SAN dysfunction in this canine model of pacing-induced AF.

Impaired SAN function in AF

AF-induced remodeling of ionic currents in the atrium has been well documented.^{17,18} Typical electrophysiologic remodeling in AF includes APD shortening, down-regulation of L-type Ca^{2+} channel ($I_{\text{Ca,L}}$) caused by atrial cardiomyocyte Ca^{2+} loading,^{19,20} down-regulation of I_{to} ,²¹ and up-regulation of I_{KACH} and I_{K1} .^{17,18} The ionic current remodeling could reduce the slope of phase 0, hyperpolarize V_m , and reduce heart rate. However, the mechanism of tachycardia-induced SAN dysfunction is unclear. Yeh et al²² recently reported that I_f down-regulation may contribute to the association between SAN dysfunction and supraventricular tachyarrhythmias. However, normal functioning SAN depends not only on membrane ionic currents but also on rhythmic Ca^{2+} releases from the SR.^{9-12,14} Compared with normal SANs, AF SANs did not exhibit spontaneous LD-CAE upon isoproterenol infusion, suggesting impaired spontaneous SR Ca^{2+} release. Caffeine, which induces SR Ca^{2+} release, results in LDCAE and heart rate acceleration in normal but not in AF dogs. In contrast to normal intact SANs whose isoproterenol response depends primarily on the ability of the superior SAN to increase LDCAE,²³ the heart rate of AF dogs was increased by acceleration of ectopic foci or inferior SAN. These findings indicate that, in addition to abnormal membrane ionic currents (the “membrane clock”), dogs with AF have significant impairment of the Ca^{2+} clock in the SAN. The abnormal membrane and Ca^{2+} clocks both are responsible for SAN dysfunction in AF. SACT was also depressed in this model, which supports the presence of SAN dysfunction in this model.

RyR2 and SAN function

This study demonstrated that the slope of LDCAE during beta-adrenergic stimulation was much shallower in AF than in normal RAs, suggesting that spontaneous SR Ca^{2+} release is impaired in AF RAs. Coupled with our observation of lower expression of RyR2 in superior SAN from AF dogs, these results suggest that down-regulation of RyR2 contributes to impaired spontaneous SR Ca^{2+} release, thus reflecting a defective Ca^{2+} clock mechanism in SAN. This conclusion is consistent with several studies that linked RyR2 dysfunction to AF and SAN dysfunction.²³⁻²⁵ Patients with a genomic deletion of RyR2 exon 3 developed catecholaminergic polymorphic ventricular tachycardia with SAN dysfunction, AF, and atrial standstill.²³ Lower expression level of RyR2 mRNA in atrial tissue from chronic AF patients has been reported.²⁴ It also has been reported that AF may cause hyperphosphorylation of RyR2 in the atria.²⁵ The hyperphosphorylation may prevent further

RyR2 phosphorylation during isoproterenol infusion, resulting in impaired SR Ca^{2+} release to isoproterenol.

Impaired response to caffeine

This study found that caffeine failed to increase Ca_i in dogs with AF. These findings may be explained by depletion of SR, depletion of SR Ca^{2+} content, and/or reduced RyR2 on the SR. Ausma et al²⁶ reported that AF initially causes Ca_i overload. However, after the initial 2 weeks of AF, the sarcolemma-bound Ca^{2+} gradually declined to a level below that at baseline. The authors suggested that persistent Ca^{2+} overload causes structural adaptation of chronic AF characterized by depletion of contractile filaments and the SR. The loss of SR could impair Ca_i elevation after caffeine, whether or not the Ca^{2+} content in the remaining SR is normal or depleted. Biochemical studies of changes in expression level of Ca^{2+} handling proteins in AF are inconsistent, depending on age, duration of AF, and variability of experimental conditions.¹⁸ This study using a canine model of pacing-induced AF demonstrated normal SERCA2a and down-regulation of RyR2. These changes may not be applicable to all AF models or to humans. Because rapid pacing is needed to induce AF in this model, these changes may be related to rapid atrial rates due to either rapid pacing or AF. Nonetheless, reduced RyR2 is consistent with impaired Ca_i elevation after caffeine.

Study limitations

Because optical action potentials collected from the canine three-dimensional SAN contain contributions from the surface and intramural layers, including the SAN, they represent a weighted average of transmembrane action potentials throughout the entire canine atrial wall.^{27,28} However, this effect was not obvious in our study. The discrepancy can be explained by the different mapping technique used. The canine SAN is located at the epicardial side and is covered by a thin fibrous membrane.^{15,29} The SAN can be dilated more than 1 mm during the perfusion state.³⁰ Because the depth of penetration of optical mapping is only 1 to 2 mm, the effect of a different mapping technique may be more obvious during SAN mapping. The high spatial resolution ($0.35 \times 0.35 \text{ mm}^2$ per pixel) of the camera allowed us to study optical signals of the SAN with little contamination from neighboring sites. In contrast, a recent study by Fedorov et al²⁸ used a 16×16 photodiode array to acquire signals from both epicardial and endocardial sites. Due to the difference in spatial resolution, the signals registered in those studies are more likely to be a mixture of SAN and the surrounding atrial structures. Therefore, a notch was consistently observed in their study, but a notch on the optical signal was not observed in this study. In addition, the effect of the double layer was mainly observed after phase 0 activation of RA, our observation of LDCAE was located before phase 0 activation of RA. Finally, despite identical imaging parameters, the same sites that did not exhibit LDCAE under basal conditions developed LDCAE after isoproterenol infusion.

The temperature of the tissue was maintained at 36.5° to 37°C without superfusion. Hypothermia alone can induce Ca^{2+} overload and SAN dysfunction. However, because the experimental condition was same between the control and AF groups, we believe the temperature difference cannot explain the SAN dysfunction and impaired Ca_i release in AF dogs.

The ectopic foci were outside the mapped field. Therefore, we do not know if Ca^{2+} clock malfunction was also present in the ectopic (latent) pacemakers. Ca^{2+} handling protein studies were limited by the short supply of RA tissues. Although the endocardial half of SAN tissue was removed, the remaining tissue still contained both pacemaking cells and non-SAN cells. Therefore, our results might have underestimated the abnormality of the ryanodine receptor changes of the SAN cells. In particular, the insufficient amount of tissue

prevented us from performing detailed biochemical assays to determine the Ca^{2+} -ATPase activity of SERCA2a and phosphorylation status of RyR2 and phospholamban.

Conclusion

SAN dysfunction in AF is associated with Ca^{2+} clock malfunction characterized by reduced SR Ca^{2+} release and down-regulated RyR2 in the superior SAN. These findings suggest that a defective Ca^{2+} clock is a mechanism of SAN dysfunction in a canine model of pacing-induced AF.

Supplementary Material

Refer to Web version on PubMed Central for supplementary material.

Acknowledgments

We thank Changyu Shen for statistics consultation.

This study was supported in part by National Institutes of Health Grants P01 HL78931, R01 HL78932, and 71140; a Korean Ministry of Information and Communication and Institute for Information Technology Advancement through research and develop support project to Dr. Joung; an AHA Established Investigator Award to Dr. Lin; a Nihon Kohden/St. Jude Medical Electrophysiology fellowship to Dr. Maruyama; Medtronic-Zipes Endowments to Dr. Chen; and a VA Young Investigator Grant and St. Jude Medical, Inc., research grant to Dr. Das. Dr. Zipes and Chen are consultants to Medtronic, Inc. Dr. Das receives research grants from St. Jude Medical. Medtronic provided equipment used in this study.

ABBREVIATIONS

AF	atrial fibrillation
APD	action potential duration
cSNRT	corrected sinoatrial node recovery time
LDCAE	late diastolic Ca_i elevation
RA	right atrium
RyR2	type 2 ryanodine receptor
SACT	sinoatrial node conduction time
SAN	sinoatrial node
SERCA2a	sarcoplasmic reticulum Ca^{2+} -ATPase 2a
SNRT	sinoatrial node recovery time
SR	sarcoplasmic reticulum

References

1. Allesie M, Ausma J, Schotten U. Electrical, contractile and structural remodeling during atrial fibrillation. *Cardiovasc Res* 2002;54:230–246. [PubMed: 12062329]
2. Gomes JA, Kang PS, Matheson M, et al. Coexistence of sick sinus rhythm and atrial flutter-fibrillation. *Circulation* 1981;63:80–86. [PubMed: 7438410]
3. Hocini M, Sanders P, Deisenhofer I, et al. Reverse remodeling of sinus node function after catheter ablation of atrial fibrillation in patients with prolonged sinus pauses. *Circulation* 2003;108:1172–1175. [PubMed: 12952840]
4. Elvan A, Wylie K, Zipes DP. Pacing-induced chronic atrial fibrillation impairs sinus node function in dogs: electrophysiological remodeling. *Circulation* 1996;94:2953–2960. [PubMed: 8941126]

5. Sparks PB, Jayaprakash S, Vohra JK, et al. Electrical remodeling of the atria associated with paroxysmal and chronic atrial flutter. *Circulation* 2000;102:1807–1813. [PubMed: 11023936]
6. Van Den Berg MP, Van GI. Atrial fibrillation and sinus node dysfunction. *J Am Coll Cardiol* 2001;38:1585–1586. [PubMed: 11691547]
7. DiFrancesco D. Pacemaker mechanisms in cardiac tissue. *Annu Rev Physiol* 1993;55:455–472. [PubMed: 7682045]
8. DiFrancesco D. The pacemaker current (I_f) plays an important role in regulating SA node pacemaker activity. *Cardiovasc Res* 1995;30:307–308. [PubMed: 7585819]
9. Hata T, Noda T, Nishimura M, et al. The role of Ca²⁺ release from sarcoplasmic reticulum in the regulation of sinoatrial node automaticity. *Heart Vessels* 1996;11:234–241. [PubMed: 9129243]
10. Ju YK, Allen DG. Intracellular calcium and Na⁺-Ca²⁺ exchange current in isolated toad pacemaker cells. *J Physiol* 1998;508(Pt 1):153–166. [PubMed: 9490832]
11. Bogdanov KY, Vinogradova TM, Lakatta EG. Sinoatrial nodal cell ryanodine receptor and Na(+)-Ca(2+) exchanger: molecular partners in pacemaker regulation. *Circ Res* 2001;88:1254–1258. [PubMed: 11420301]
12. Vinogradova TM, Bogdanov KY, Lakatta EG. beta-Adrenergic stimulation modulates ryanodine receptor Ca(2+) release during diastolic depolarization to accelerate pacemaker activity in rabbit sinoatrial nodal cells. *Circ Res* 2002;90:73–79. [PubMed: 11786521]
13. Vinogradova TM, Zhou YY, Maltsev V, et al. Rhythmic ryanodine receptor Ca²⁺ releases during diastolic depolarization of sinoatrial pacemaker cells do not require membrane depolarization. *Circ Res* 2004;94:802–809. [PubMed: 14963011]
14. Vinogradova TM, Lyashkov AE, Zhu W, et al. High basal protein kinase A-dependent phosphorylation drives rhythmic internal Ca²⁺ store oscillations and spontaneous beating of cardiac pacemaker cells. *Circ Res* 2006;98:505–514. [PubMed: 16424365]
15. Joung B, Tang L, Maruyama M, et al. Intracellular calcium dynamics and the acceleration of sinus rhythm by beta-adrenergic stimulation. *Circulation* 2009;119:788–796. [PubMed: 19188501]
16. Narula OS, Shantha N, Vasquez M, et al. A new method for measurement of sinoatrial conduction time. *Circulation* 1978;58:706–714. [PubMed: 688581]
17. Verkerk AO, Wilders R, Coronel R, et al. Ionic remodeling of sinoatrial node cells by heart failure. *Circulation* 2003;108:760–766. [PubMed: 12885752]
18. Nattel S, Maguy A, Le BS, et al. Arrhythmogenic ion-channel remodeling in the heart: heart failure, myocardial infarction, and atrial fibrillation. *Physiol Rev* 2007;87:425–456. [PubMed: 17429037]
19. Van Wagoner DR, Pond AL, Lamorgese M, et al. Atrial L-type Ca²⁺ currents and human atrial fibrillation. *Circ Res* 1999;85:428–436. [PubMed: 10473672]
20. Workman AJ, Kane KA, Rankin AC. The contribution of ionic currents to changes in refractoriness of human atrial myocytes associated with chronic atrial fibrillation. *Cardiovasc Res* 2001;52:226–235. [PubMed: 11684070]
21. Van Wagoner DR, Pond AL, McCarthy PM, et al. Outward K⁺ current densities and Kv1.5 expression are reduced in chronic human atrial fibrillation. *Circ Res* 1997;80:772–781. [PubMed: 9168779]
22. Yeh YH, Burstein B, Qi XY, et al. Funny current downregulation and sinus node dysfunction associated with atrial tachyarrhythmia: a molecular basis for tachycardiabradycardia syndrome. *Circulation* 2009;119:1576–1585. [PubMed: 19289641]
23. Bhuiyan ZA, Van Den Berg MP, van Tintelen JP, et al. Expanding spectrum of human RYR2-related disease: new electrocardiographic, structural, and genetic features. *Circulation* 2007;116:1569–1576. [PubMed: 17875969]
24. Ohkusa T, Ueyama T, Yamada J, et al. Alterations in cardiac sarcoplasmic reticulum Ca²⁺ regulatory proteins in the atrial tissue of patients with chronic atrial fibrillation. *J Am Coll Cardiol* 1999;34:255–263. [PubMed: 10400019]
25. Vest JA, Wehrens XH, Reiken SR, et al. Defective cardiac ryanodine receptor regulation during atrial fibrillation. *Circulation* 2005;111:2025–2032. [PubMed: 15851612]
26. Ausma J, Dispersyn GD, Duimel H, et al. Changes in ultrastructural calcium distribution in goat atria during atrial fibrillation. *J Mol Cell Cardiol* 2000;32:355–364. [PubMed: 10731435]

27. Fedorov VV, Lozinsky IT, Sosunov EA, et al. Application of blebbistatin as an excitation-contraction uncoupler for electrophysiologic study of rat and rabbit hearts. *Heart Rhythm* 2007;4:619–626. [PubMed: 17467631]
28. Fedorov VV, Schuessler RB, Hemphill M, et al. Structural and functional evidence for discrete exit pathways that connect the canine sinoatrial node and atria. *Circ Res* 2009;104:915–923. [PubMed: 19246679]
29. Woods WT, Urthaler F, James TN. Spontaneous action potentials of cells in the canine sinus node. *Circ Res* 1976;39:76–82. [PubMed: 1277407]
30. James TN. Structure and function of the sinus node, AV node and his bundle of the human heart: part II—function. *Prog Cardiovasc Dis* 2003;45:327–360. [PubMed: 12638096]

Appendix Supplementary data

Supplementary data associated with this article can be found, in the online version, at doi: 10.1016/j.hrthm.2009.09.018.

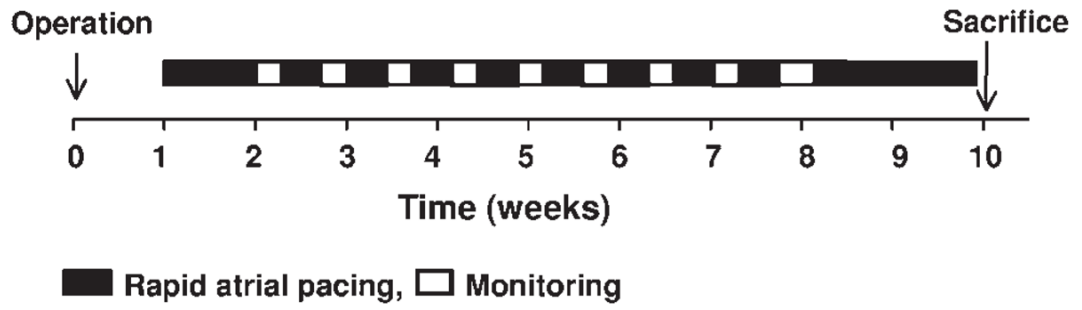


Figure 1.
Experimental protocol for induction of atrial fibrillation.

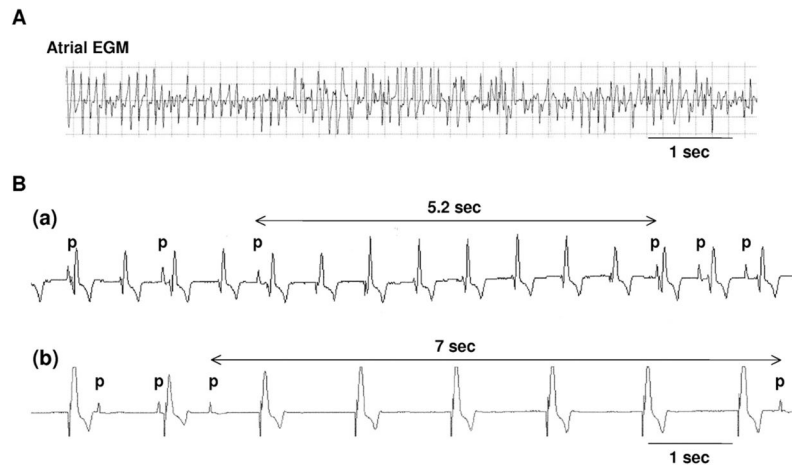


Figure 2. Atrial fibrillation and sinoatrial node dysfunction *in vivo*. **A:** Stored atrial electrogram (EGM) showing atrial fibrillation. **B:** Sinus pauses documented by Holter monitoring. **(a)** Sinus pause of 5.2 seconds during ventricular pacing at 90 bpm. **(b)** Sinus pause of 7 seconds during ventricular pacing at 50 bpm. p = P wave.

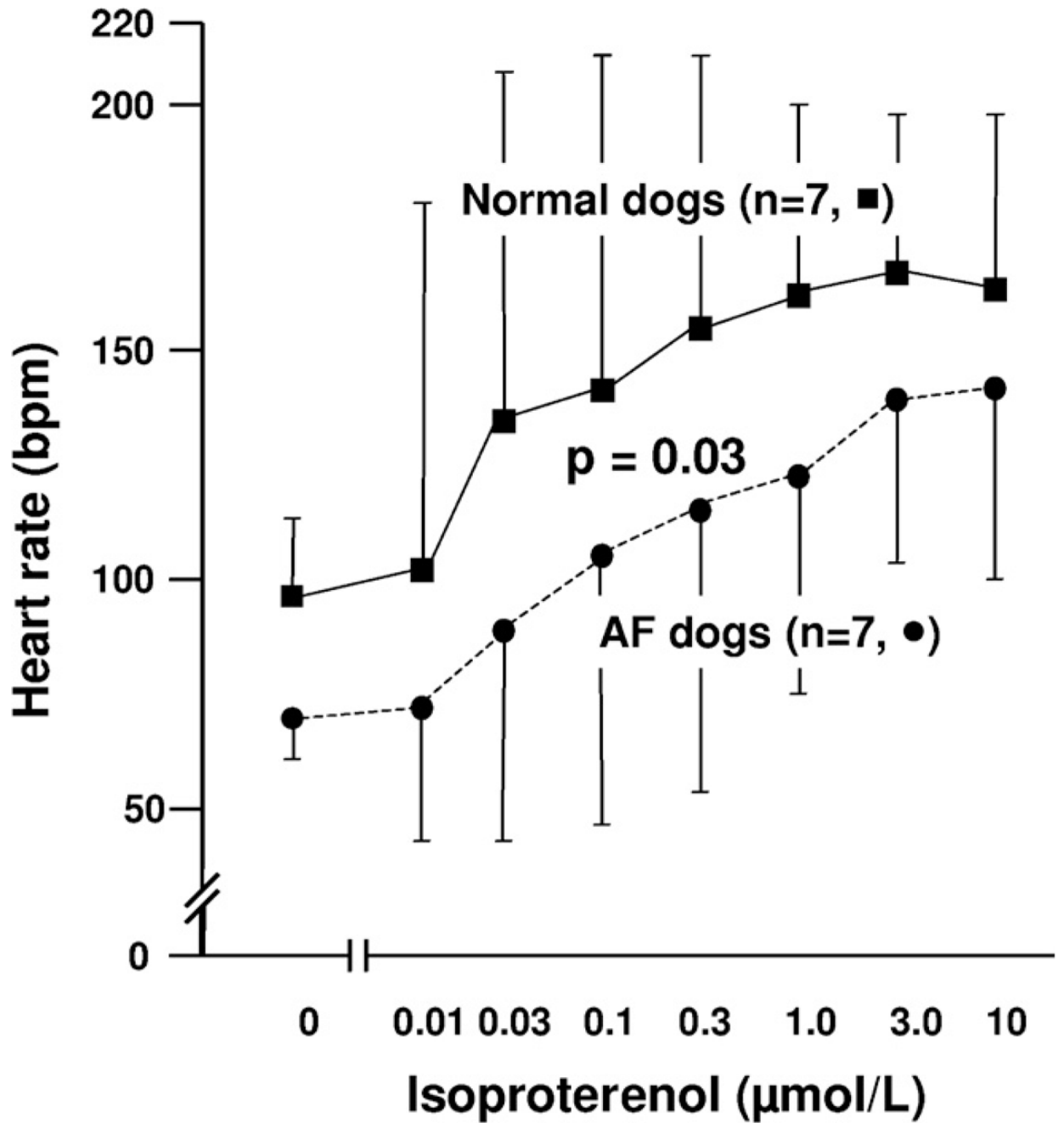


Figure 3. Impaired isoproterenol-induced heart rate increase in right atria (RA) from atrial fibrillation (AF) dogs. Isoproterenol dose–response curve was determined for 7 normal and 7 AF dogs. Compared to normal RA (*squares*), AF RA (*circles*) showed significantly impaired heart rate increase during isoproterenol infusion ($P = .03$).

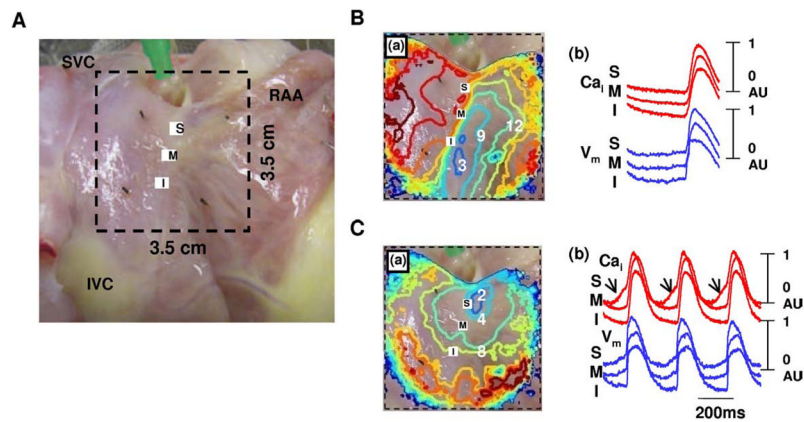


Figure 4. Isoproterenol response of normal dogs. **A:** Epicardial photographs of perfused right atrial (RA) preparation with 35×35 -mm optical field of view. **B:** Baseline. **C:** Isoproterenol infusion of $0.3 \mu\text{mol/L}$. (a) RA V_m isochronal map. (b) Ca_i (red) and V_m (blue) tracings from superior (S), mid (M), and inferior (I) sinoatrial nodes. Note heart rate increase and shifting of the leading pacemaker site to the superior sinoatrial node with robust late diastolic Ca_i elevation (arrows). The unit of numbers on the RA V_m isochronal map is milliseconds. Earliest activation of the RA was considered as 0 ms. IVC = inferior vena cava; RAA = right atrial appendage; SVC = superior vena cava.

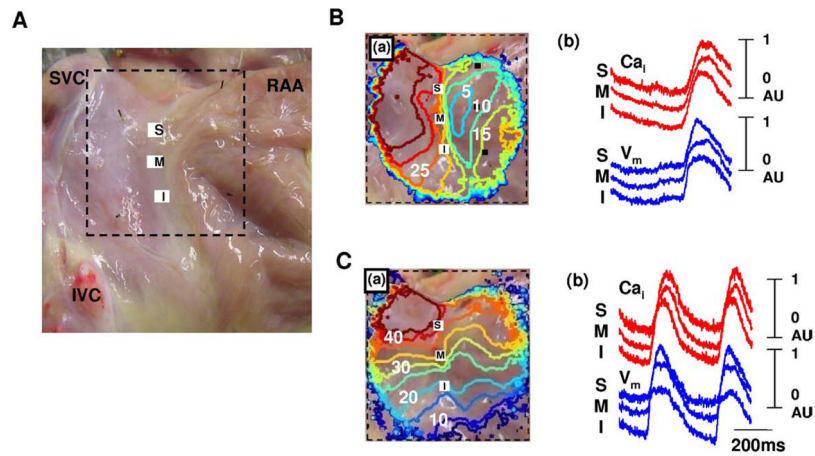


Figure 5. Complete absence of late diastolic Ca_i elevation in atrial fibrillation dogs during isoproterenol infusion. **A:** Epicardial photograph of a perfused right atrial (RA) preparation with 35×35 -mm optical fields of view. **B:** Baseline. **C:** Isoproterenol infusion of $1.0 \mu\text{mol/L}$. (a) RA V_m isochronal map. (b) Ca_i (red) and V_m (blue) tracings from superior (S), mid (M), and inferior (I) sinoatrial nodes. Late diastolic Ca_i elevation was not observed at any dosage of isoproterenol infusion. The unit of numbers on the RA V_m isochronal map is milliseconds. Earliest activation of the RA was considered as 0 ms. IVC = inferior vena cava; RAA = right atrial appendage; SVC = superior vena cava.

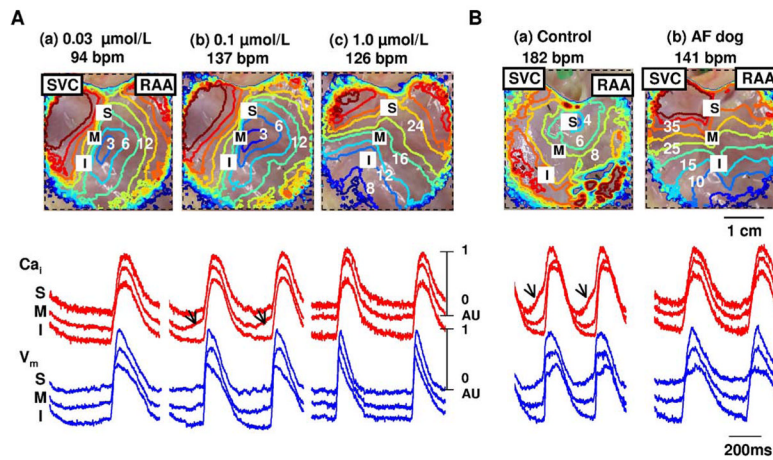


Figure 6.

A: Transient late diastolic Ca_i elevation (LDCAE) in atrial fibrillation (AF) dogs during isoproterenol infusion. (a)–(c) show isoproterenol infusion of 0.03, 0.1, and 1.0 μmol/L, respectively. (a) Note isoproterenol-induced LDCAE at mid sinoatrial node (*arrows*) during isoproterenol infusion of 0.1 μmol/L. (c) Rhythm was generated from the inferior right atrium (RA). **B:** Complete absence of LDCAE in AF dogs during caffeine bolus injection. (a) Caffeine response in normal RA. Note increase of heart rate and superior shift of the leading pacemaker site with robust LDCAE (*arrows*). (b) Caffeine responses in AF RA. There was no LDCAE from the sinoatrial node. Heart rate was increased by acceleration of ectopic focus. **Upper panels** show RA V_m isochronal maps. **Lower panels** show Ca_i (*red*) and V_m (*blue*) tracings from superior (S), mid (M), and inferior (I) sinoatrial nodes, respectively. The unit of numbers on the RA V_m isochronal map is milliseconds. Earliest activation of the RA was considered as 0 ms. RAA = right atrial appendage; SVC = superior vena cava.

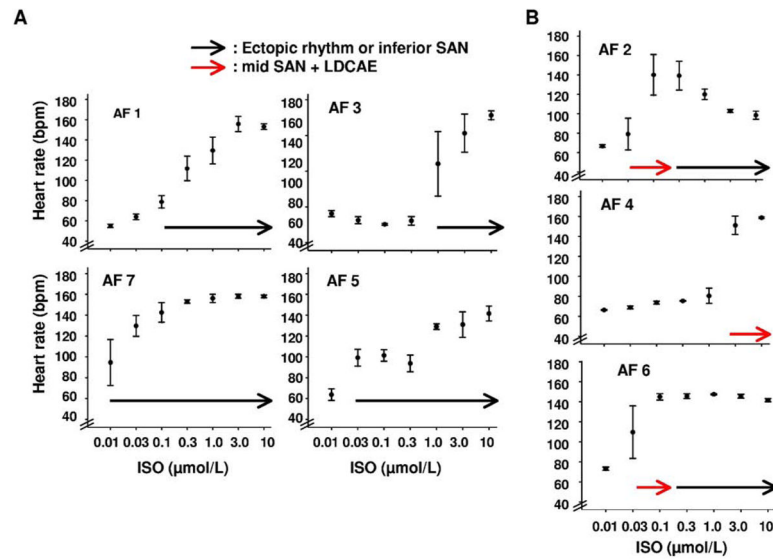


Figure 7. Origin of heart rhythm during acceleration of heart rate in each of the seven right atria (RAs) from atrial fibrillation (AF) dogs. **A:** AF RA without late diastolic Ca_i elevation (LDCAE) ($n = 4$). Note heart rate increase by acceleration of ectopic foci or inferior sinoatrial node (SAN) (*black arrow*). **B:** AF RA with transient LDCAE ($n = 3$). Note heart rate increase by LDCAE from mid SAN (*red arrow*). ISO = isoproterenol.

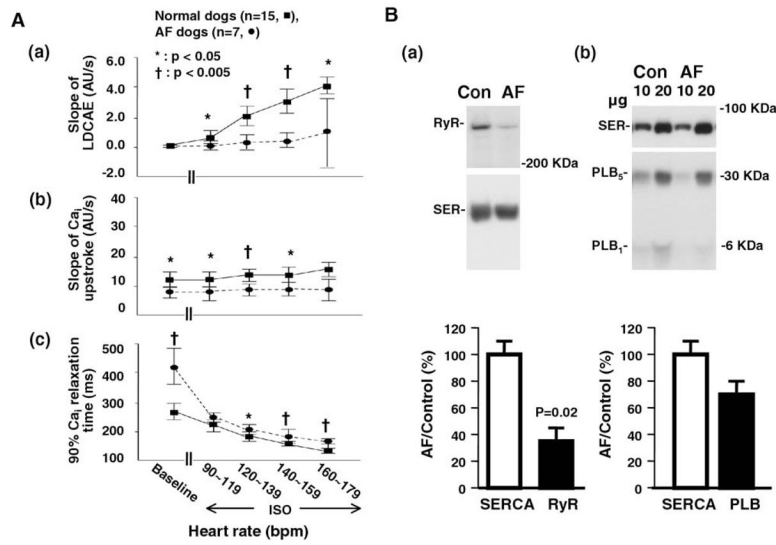


Figure 8. Impaired sarcoplasmic reticulum Ca²⁺ handling in atrial fibrillation (AF) dogs. **A:** Comparison of (a) slope of late diastolic Ca_i elevation (LDCAE), (b) slope of Ca_i upstroke, and (c) 90% Ca_i relaxation time measured from the superior sinoatrial node between normal and AF dogs at baseline and isoproterenol infusion. Responses after isoproterenol infusion are grouped by heart rate. **B:** Comparison of (a) sarcoplasmic reticulum Ca²⁺-ATPase 2a (SERCA2a) and ryanodine receptor (RyR) and (b) SERCA2a and phospholamban (PLB) at the superior sinoatrial node between normal and AF dogs. **Upper** and **lower panels** show representative immunoblot and relative values, respectively.